Oxidation kinetics in SrTiO₃ homoepitaxy on SrTiO₃(001)

X. D. Zhu[a)]
Department of Physics, University of California–Davis, Davis, California 95616

Weidong Si and X. X. Xi
Department of Physics, The Penn State University, University Park, Pennsylvania 16802

Qidu Jiang
Department of Chemistry, University of Houston, Houston, Texas 77204-5641

Using an oblique-incidence optical reflectivity difference technique, we investigated kinetic processes in SrTiO₃ homoepitaxy on SrTiO₃(001) under pulsed-laser deposition conditions. Depending upon growth temperature and oxygen ambient pressure, we found that the oxidation of an as-grown SrTiO₃ monolayer may take a much longer time to complete than the recrystallization of the monolayer. The oxidation reaction was found to be characterized by an effective activation energy barrier of 1.35 eV and a large preexponential factor. © *2001 American Institute of Physics.*
[DOI: 10.1063/1.1338497]

Two-dimensional epitaxy of thin-film oxides has been a subject of intense research as the atomic-level control of surfaces and interfaces is recognized to be essential for various oxide-based heterostructure devices.[1,2] So far, most efforts have been focused on the crystalline structure or recrystallization of epitaxially grown films. *In situ* reflection high-energy electron diffraction (RHEED) from the growth surface has been successfully used in these efforts.[1–6] For example, the oscillation of the RHEED intensities during a continuous deposition is used as the indicator of layer-by-layer growth (through nucleation, growth, and coalescence in two dimensions). At high temperatures, the disappearance of RHEED intensity oscillations is used as an indicator of step-flow growth.[7] The short-time and long-time recovery of the RHEED intensities in an interrupted deposition are used to monitor the temporal evolution of recrystallization.

In addition to crystallinity, the properties of oxide films are subject to oxygen stoichiometry.[8–11] In most oxide epitaxy, the full oxygenation of an oxide film is achieved through postdeposition cooling treatments under high pressure of an oxidant, regardless of the origins of the initial incomplete oxygenation. The latter can result from the thermodynamic conditions such as substrate temperature and ambient oxidant partial pressure *during growth* and from kinetic conditions such as the rate of deposition. At a high rate of deposition, the oxidation of an as-deposited oxide film *during growth* may be incomplete. This aspect has not been studied in the context of oxide epitaxy, presumably because most commonly used *in situ* monitoring techniques cannot probe the oxidation state of an oxide film with *submonolayer* sensitivity.

Photoemission studies by many groups show that oxygen deficiency in a SrTiO₃ crystal is mostly in the form of oxygen vacancies.[12,13] The SrTiO₃ crystal has a direct energy gap of 3.4 eV separating the top of the O 2*p* valence band from the bottom of the Ti 3*d* conduction band.[14] The Fermi level is very close to the bottom of the conduction band.

Upon annealing at high temperatures in vacuum, a stoichiometric SrTiO₃ crystal loses oxygen (starting from the surface region) and oxygen vacancies are formed, mostly in TiO₂ layers.[12,13,15] As a result, a new energy state develops in the energy gap at 1.2–1.4 eV below the bottom of the Ti 3*d* conduction band. This new energy state, having the Ti 3*d* orbital character, causes a vacuum-annealed or ''reduced'' SrTiO₃ crystal to be absorptive in the visible range. Since the oxygen deficiency in a SrTiO₃ crystalline film is accompanied by the appearance of optical absorption in the visible, one can detect the state and kinetics of oxidation of an epitaxially grown SrTiO₃ monolayer by monitoring the absorption of the monolayer *during growth*.

In this letter, we report an investigation of the oxidation kinetics in SrTiO₃ (STO) homoepitaxy on SrTiO₃(001) using an oblique-incidence optical reflectivity difference technique.[16–19] We follow the postdeposition evolution of the optical dielectric constant ϵ_d of an as-deposited STO monolayer film. ϵ_d deviates initially from the dielectric constant ϵ_s for a stoichiometric SrTiO₃ substrate by $\delta\epsilon_d = \delta\epsilon_d' + i\,\delta\epsilon_d''$. Since the stoichiometric SrTiO₃ is transparent in the visible range, the imaginary part $\delta\epsilon_d''$ that characterizes the absorption in the visible comes from the incomplete oxidation of the monolayer film.[20,21]

Our experiment is performed in a pulsed-laser deposition chamber with a base pressure of 1×10^{-6} Torr. A SrTiO₃(001) single-crystal plate is used as the substrate. It is preannealed in an oxygen flow at 1100 °C for 4 h. The scanning tunneling microscopy image shows that the annealed SrTiO₃(001) surface exhibits terraces with heights predominantly of 0.4 nm (one unit cell) and widths of 300 nm. A small portion of the surface is covered with terraces of 0.2 nm in height. All terraces are atomically flat with corrugation less than 0.1 nm. The substrate temperature during growth is variable from 270 to 900 °C. During growth, the oxygen pressure can be varied from 1×10^{-5} Torr to a few Torr. For deposition, we use the laser ablation of a stoichiometric SrTiO₃ target with optical pulses from a 248 nm KrF excimer laser operated at a repetition rate of 5 Hz. The single pulse energy is 550 mJ and the energy density on the target

---

a)Electronic mail: xdzhu@physics.ucdavis.edu

is 1.5 J/cm^2. The average deposition rate is calibrated to be 0.36 ML per second at oxygen pressure of 100 mTorr and 0.5 ML per second at 0.3 mTorr.

For the optical reflectivity difference measurement, we use a 2 mW He–Ne laser at $\lambda = 633$ nm as the probe. At the photon energy of 1.96 eV, the 1-mm-thick SrTiO$_3$ substrate is transparent and has a real dielectric constant $\epsilon_s = 5.66$. The laser is initially p polarized. We alter the polarization of the laser beam from p to s polarization at a rate of $\Omega = 50$ kHz with a photoelastic modulator (PEM-90, Hinds Instruments). The polarization-modulated beam is incident on the SrTiO$_3$(001) substrate at an angle of $\phi_{\mathrm{inc}} = 60°$. We pass the reflected beam through an analyzing polarizer with its transmission axis at an angle of θ from the s polarization. The resultant beam intensity $I_r(t)$ is detected with a photodiode. $I_r(t)$ has terms that vary with time at various harmonics of the modulation frequency Ω. We detect the second harmonics $I_r(2\Omega)\cos(2\Omega t)$.

Let $r_{p0} = |r_{p0}|\exp(i\Phi_{p0})$ and $r_{s0} = |r_{s0}|\exp(i\Phi_{s0})$ be the reflection coefficients for p- and s-polarized light from the substrate before deposition. And let $r_p = |r_p|\exp(i\Phi_p)$ and $r_s = |r_s|\exp(i\Phi_s)$ be the reflection coefficients after an oxide layer is deposited on the substrate. We adjust θ initially such that before deposition $I_r(2\Omega) = 0$. During the subsequent deposition, the change in $I_r(2\Omega)$ is given by[16–19]

$$I_r(2\Omega) \cong I_{\mathrm{inc}}|r_{p0}\sin\theta|^2\,\mathrm{Re}\{\Delta_p - \Delta_s\}, \tag{1}$$

where $\Delta_p \equiv (r_p - r_{p0})/r_{p0}$ and $\Delta_s \equiv (r_s - r_{s0})/r_{s0}$. It can be shown that[16]

$$\delta\epsilon_d = \delta\epsilon'_d + i\epsilon''_d$$
$$= (-i)\left\{ \frac{\lambda[\epsilon_s^2\cos^2\phi_{\mathrm{inc}} - (\epsilon_s - \sin^2\phi_{\mathrm{inc}})]}{4\pi d\cos\phi_{\mathrm{inc}}\sin^2\phi_{\mathrm{inc}}(\epsilon_s - 1)} \right\}(\Delta_p - \Delta_s), \tag{2}$$

where d is the averaged thickness of the deposited layer. As a result, $\delta\epsilon''_d$ is monitored through the measurement of $I_r(2\Omega)$. Since the photon energy of 1.96 eV is large compared to the energy separation (1.2–1.4 eV) between the occupied oxygen-vacancy-induced state and the bottom of the conduction band, $\delta\epsilon''_d$ is associated with oxygen vacancies in the as-grown STO monolayer.

In our measurement, we deposit 1 ML of SrTiO$_3$ ($d = 0.39$ nm in height) on the SrTiO$_3$(001) substrate and follow the change and recovery of $\delta\epsilon''_d$. To deduce the kinetics parameters of the oxidation, we studied the dependence of the recovery rate for $\delta\epsilon''_d$ on oxygen pressure and substrate temperature. In Figs. 1(a) and 1(b), we display $\delta\epsilon''_d$ before and after the deposition of a STO monolayer at oxygen pressures of 5 and 0.3 mTorr, respectively. The initial change in $\delta\epsilon''_d$ is roughly 0.4, so that $\delta\epsilon''_d/\epsilon_s = 7\%$. Comparing Fig. 1(b) with Fig. 1(a), we note that the recovery of $\delta\epsilon''_d$, for example, at 550 °C slows down dramatically when the oxygen pressure is reduced from 5 to 0.3 mTorr. The oxygen pressure dependence confirms that the kinetic process responsible for the change in $\delta\epsilon''_d$ has to do with the interaction or reaction of ambient molecular oxygen with the deposited STO monolayer. At a fixed oxygen pressure, the decay rate for $\delta\epsilon''_d$ increases with the substrate temperature, indicating that the process is also thermally activated.
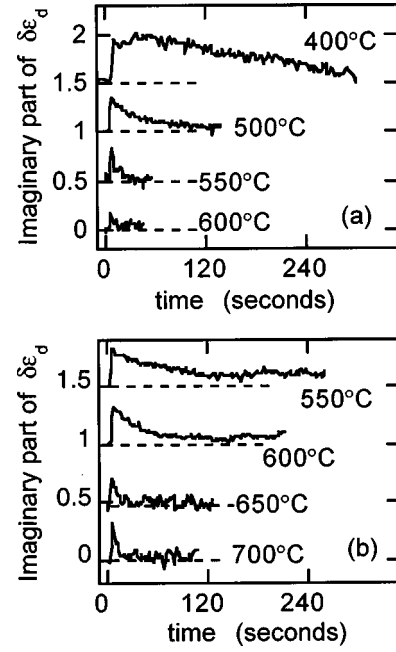
FIG. 1. Imaginary part of the optical dielectric constant $\delta\epsilon''_d$ for a deposited STO monolayer on SrTiO$_3$(001) before and after the deposition in an ambient oxygen pressure of (a) 5 mTorr and (b) 0.3 mTorr. The substrate temperature ranges between 400 and 600 °C. For display, the curves are shifted from each other by 0.5, as indicated by the dotted lines.

To extract the kinetic parameters that characterize the decay, we fit the temporal profiles of the optical signals with single-exponential functions of time $\delta\epsilon''_d \sim \exp[-\alpha(T, P_{O_2})t]$. In Fig. 2 we display the Arrhenius plots of the exponents $\alpha(T, P_{O_2})$. $\alpha(T, P_{O_2})$ are fit to Arrhenius form $\alpha(T, P_{O_2}) = \alpha(P_{O_2})\exp[-E_a/k_BT]$. At $P_{O_2} = 0.3$ mTorr, we find $E_a = 30$ kcal/mol or 1.3 eV, and $\alpha(P_{O_2} = 0.3$ mTorr$) = 1\times10^6$ s^{-1}. At $P_{O_2} = 5$ mTorr, we find $E_a = 32$ kcal/mol or 1.4 eV, and $\alpha(P_{O_2} = 5$ mTorr$) = 2\times10^7$ s^{-1}. The two Arrhenius plots can be combined roughly into a single expression:

$$\alpha(T, P_{O_2}) = 4\times10^9 \ \mathrm{Torr}^{-1}\mathrm{s}^{-1}P_{O_2}\exp[-1.35 \ \mathrm{eV}/k_BT]. \tag{3}$$

We now discuss our experimental findings. The oxygen stoichiometry effect in bulk STO has been extensively studied.[12,13,15,21] The oxygen deficiency in STO leads to doubly ionized oxygen vacancies in the TiO$_2$ layers presumably as well as free electrons. This results in optical absorption in
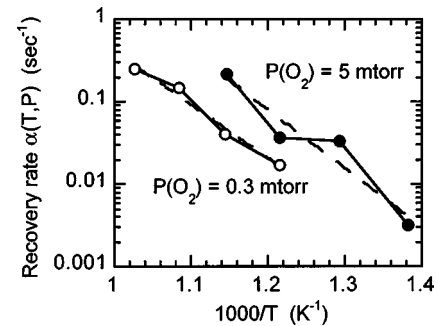
FIG. 2. Arrhenius plots of decay rates $\alpha(T, P_{O_2})$ in oxygen pressures of 5 mTorr (solid circles) and 0.3 mTorr (open circles), respectively. The dash lines are fits to Arrhenius function $\alpha(T, P_{O_2}) = \alpha(P_{O_2})\exp[-E_a/k_BT]$.

the visible range. In our present study this effect is observed at the monolayer level *during growth*. Immediately after the deposition, the as-grown STO monolayer has a very high degree of oxygen deficiency compared to the stoichiometric substrate. The high degree of oxygen deficiency is evidenced by the large initial magnitude of $\epsilon_d'' = \delta\epsilon_d'' \approx 0.4$ for the as-grown STO monolayer. It corresponds to an optical penetration depth of $l_d = 0.5 \times 10^{-4}$ cm at $\lambda = 633$ nm. This means that the *effective* volume density of oxygen vacancies in the as-grown STO monolayer is initially over 2000 times higher than that in the substrate under the growth condition.

We use a simple kinetic model to describe the oxidation of an as-grown STO monolayer on SrTiO$_3$(001). The model reproduces the observed temperature and the oxygen pressure dependence of the decay rate for $\delta\epsilon_d''$. We assume that $\delta\epsilon_d''$ of the STO monolayer is proportional to the surface density of oxygen vacancies N_v so that the recovery of the optical signal describes the decay of N_v. Since the decay rate depends on the substrate temperature, oxygen vacancies in the deposited oxide monolayer must react with oxygen adatoms (in a precursor state) rather than with ambient oxygen molecules directly. It is thus reasonable to assume that ambient oxygen molecules first dissociate into oxygen adatoms in a precursor state.[22] The oxygen adatoms (already thermally equilibrated with the substrate) either desorb from the precursor state or react with the nearby oxygen vacancies (either directly or through oxygen vacancy conduction). Let N_i be the surface density of oxygen adatoms in the precursor state. The rate of change for N_i equals the rate of dissociative adsorption for ambient molecular oxygen minus the rate of desorption for oxygen adatoms from the precursor state and the rate at which these oxygen adatoms react with the nearby oxygen vacancies,

$$\frac{dN_i}{dt} = S\Gamma_p\left[\frac{(N_{v0}-N_v)-N_i}{N_s}\right] - \nu_{des}N_i\exp(-E_{des}/k_BT)$$
$$- \nu_R N_i \exp(-E_R/k_BT), \qquad (4)$$

where N_{v0} is the surface density of oxygen vacancies immediately after the deposition. The rate of change for N_v as a result of oxidation is given by

$$\frac{dN_v}{dt} = -\nu_R N_i \exp(-E_R/k_BT), \qquad (5)$$

where $\Gamma_p = P_{O_2}/\sqrt{2\pi M_{O_2}k_BT_g}$ is the surface collision rate for ambient molecular oxygen at room temperature T_g. M_{O_2} is the mass of an oxygen molecule. N_s is the maximally possible density for surface oxygen vacancies. $[(N_{v0}-N_v) - N_i]/N_s$ is the probability for an oxygen molecule to strike an unoccupied oxygen vacancy site and S is the sticking probability or the probability that such an oxygen molecule successfully dissociates into two precursor state oxygen adatoms. ν_{des} and E_{des} are the preexponential factor and the energy barrier for an adsorbed oxygen atom to desorb from the precursor state, respectively. ν_R and E_R are the preexponential factor and the energy barrier for an adsorbed oxygen atom to react with the nearby oxygen vacancy, respectively. Since the rate of change for N_v is roughly proportional to the ambient oxygen pressure, it suggests that $N_s\nu_{des}\exp(-E_{des}/k_BT) \gg S\Gamma_p$ and the reaction rate is small compared

to the desorption rate. As a result, we obtain a quasi-steady-state density for N_i as $N_i \approx [S\Gamma_p(N_{v0}-N_v)/N_s\nu_{des}] \times \exp(E_{des}/k_BT)$ from Eq. (4). Solving Eq. (5), we arrive at $N_v \cong N_{v0}\exp[-\alpha(P_{O_2},T)t]$. The exponent $\alpha(P_{O_2},T) = (S\Gamma_p/N_s)(\nu_R/\nu_{des})\exp[-(E_R-E_{des})/k_BT]$ is an Arrhenius function of temperature and has a nearly linear dependence on the oxygen pressure. Since $\delta\epsilon_d'' \propto N_v$, the recovery of the optical signal is expected to evolve also as $\exp[-\alpha(P_{O_2},T)t]$. This is what we observed experimentally. This model suggests that the experimentally measured energy barrier is the difference between that for a precursor state oxygen atom to react with a nearby oxygen vacancy and the barrier for desorption, $E_a = E_R - E_{des} = 1.35$ eV.

The main conclusion from our study is that depending upon the substrate temperature and oxygen pressure, even long after the oxide film is recrystallized, the oxygen stoichiometry and the resultant properties of the film may be far from restored to those of a stoichiometric STO crystal.

[1] M. E. Klausmeier-Brown, G. F. Virshup, I. Bozovic, J. N. Eckstein, and K. S. Ralls, Appl. Phys. Lett. **60**, 2806 (1992).
[2] M. Kawasaki, K. Takahashi, T. Maeda, R. Tsuchiya, M. Shinohara, O. Ishiyama, T. Yonezawa, M. Yoshimoto, and H. Koinuma, Science **266**, 1540 (1994).
[3] G. Koster, G. J. H. Rijnders, D. H. A. Blank, and H. Rogalla, Appl. Phys. Lett. **74**, 3729 (1999).
[4] M. Lippmaa, N. Nakagawa, M. Kawasaki, S. Ohashi, Y. Inaguma, M. Itoh, and H. Koinuma, Appl. Phys. Lett. **74**, 3543 (1999).
[5] H. Karl and B. Stritzker, Phys. Rev. Lett. **69**, 2939 (1992).
[6] I. Bozovic and J. N. Eckstein, Appl. Surf. Sci. **113**, 189 (1997).
[7] J. H. Neave, P. J. Dobson, B. A. Joyce, and J. Zhang, Appl. Phys. Lett. **47**, 100 (1985).
[8] H. L. Ju, J. Gopalakrishnan, J. L. Peng, Qi Li, G. C. Xiong, T. Venkatesan, and R. L. Greene, Phys. Rev. B **51**, 6143 (1995).
[9] R. Waser and D. M. Smyth, in *Ferroelectric Thin Films: Synthesis and Basic Properties*, edited by C. P. de Araujo, J. F. Scott, and G. W. Taylor (Gordon and Breach, Amsterdam, 1996), p. 47.
[10] J. P. Sydow, R. A. Buhrman, and B. H. Moeckly, Appl. Phys. Lett. **72**, 3512 (1998).
[11] W. Si, H.-C. Li, and X. X. Xi, Appl. Phys. Lett. **74**, 2839 (1999).
[12] A. Hirata, A. Ando, K. Saiki, and A. Koma, Surf. Sci. **310**, 89 (1994).
[13] S. Kimura, J. Yamauchi, M. Tsukuda, and S. Watanabe, Phys. Rev. B **51**, 11049 (1995).
[14] Y. Tezuka, S. Shin, T. Ishii, T. Ejima, S. Suzuki, and S. Sato, J. Phys. Soc. Jpn. **63**, 347 (1994).
[15] T. Tambo, K. Maeda, A. Shimizu, and C. Tatsuyama, J. Appl. Phys. **86**, 3213 (1999).
[16] A. Wong and X. D. Zhu, Appl. Phys. A: Mater. Sci. Process. **63**, 1 (1996).
[17] X. D. Zhu, H. B. Lu, G.-Z. Yang, Z.-Y. Li, B.-Y. Gu, and D.-Z. Zhang, Phys. Rev. B **57**, 2514 (1998).
[18] X. D. Zhu, W. Si, X. X. Xi, Qi Li, Q. D. Jiang, and M. G. Medici, Appl. Phys. Lett. **74**, 3540 (1999).
[19] X. D. Zhu and E. Nabighian, Appl. Phys. Lett. **73**, 2736 (1998).
[20] W. S. Bear, Phys. Rev. B **144**, 734 (1964).
[21] N. Chan, R. K. Sharma, and D. M. Smyth, J. Electrochem. Soc. **128**, 1762 (1981).
[22] E. B. de Mongeot, M. Rocca, and U. Valbusa, Surf. Sci. **363**, 68 (1996).